

High-Frequency Trading on Decentralized On-Chain Exchanges

Liyi Zhou ^{*}, Kaihua Qin ^{*}, Christof Ferreira Torres [†], Duc V Le [‡] and Arthur Gervais ^{*}

^{*}Imperial College London, United Kingdom

[†]University of Luxembourg, Luxembourg

[‡]Purdue University, United States

Abstract—Decentralized exchanges (DEXs) allow parties to participate in financial markets while retaining full custody of their funds. However, the transparency of blockchain-based DEX in combination with the latency for transactions to be processed, makes market-manipulation feasible. For instance, adversaries could perform *front-running* — the practice of exploiting (typically non-public) information that may change the price of an asset for financial gain.

In this work we formalize, analytically exposit and empirically evaluate an augmented variant of front-running: *sandwich attacks*, which involve front- and back-running victim transactions on a blockchain-based DEX. We quantify the probability of an adversarial trader being able to undertake the attack, based on the relative positioning of a transaction within a blockchain block. We find that a single adversarial trader can earn a daily revenue of over several thousand USD when performing sandwich attacks on one particular DEX — Uniswap, an exchange with over 5M USD daily trading volume by June 2020. In addition to a single-adversary game, we simulate the outcome of sandwich attacks under multiple competing adversaries, to account for the real-world trading environment.

I. INTRODUCTION

Decades of asset trading on traditional exchanges have brought to fruition a veritable collection of market manipulation techniques, such as front-running [6], pump and dump schemes [54] and wash trading [3]. In the context of cryptocurrencies, research to date indicates that the ecosystem requires a greater awareness of such malpractices [54], [21], [45], and better exchange design [12] to prevent misbehavior. Most existing legislation does not regulate crypto-exchanges to the same degree as traditional exchanges — leaving ignorant traders open to exploitation by predatory practices, some of which is close to risk-free.

Decentralized exchanges (DEXs) allow traders to trade financial assets without giving up asset custody to a third party. Orders can be placed and matched in their entirety through immutable blockchain smart contracts, offering the possibility of censorship resistance, where orders cannot be modified prior and after execution¹.

Disclosure: Arthur Gervais works on the Liquidity Network, a community-driven, open source layer-2 blockchain scaling solution.

¹DEX prevent anyone from censoring trades, even the exchange itself. Censorship-resistance is a key property of permissionless blockchains such as Bitcoin and Ethereum, where users remain custodian over their assets at any point in time.

Censorship-resistant trade is itself made possible through reliance on an underlying blockchain, which makes public all attempted and executed trades within its peer-to-peer (P2P) network. The transparency of the blockchain layer, however, in combination with the latency for orders to deterministically execute makes, front-running easier to undertake — and hence influences negatively the security of the trader's assets.

This paper. We focus on a combination of front- and back-running², known as a *sandwiching*, for a single on-chain DEX. To the best of our knowledge, we are the first to formalize and quantify sandwich attacks. To make their sandwich, a predatory trader first observes a blockchain P2P network for a victim transaction and then rushes to squeeze it by placing one order just before the transaction (i.e. front-run) and one order just after it (i.e. back-run). If the target transaction is going to increase (decrease) the price of an asset, the adversary can place an order before which buys (sells) the asset in question, and an order afterward which sells (buys) the asset again.

We restrict our focus to *automated market maker* (AMM) DEXs [52], [4], as opposed to DEXs which operate limit order books (LOB) [20], on account of their deterministic nature which enables us to rely on fewer assumptions in our analysis. AMM DEXs simplify trading by algorithmically performing market making³, resulting in near-instant liquidity (i.e. the ability to purchase and sell assets) for market participants. Uniswap is a prominent example of an AMM DEX, which, by March 2020, has amassed a total liquidity of nearly 48M USD (corresponding to a 75% market liquidity share for AMM DEX) and had a trading volume of over 250M USD since its inception in November 2018. We formalize, analytically exposit and empirically evaluate *sandwiching* on AMM DEXs. We quantify optimal adversarial revenues and perform a real-world empirical evaluation of sandwich attacks. We also study the probability of a transaction having a particular relative position within a blockchain block, informing the prospects for such an attack. Finally, to account for a real-world scenario in which multiple adversaries are likely to

²While the SEC defines front-running as an action on *private* information, we only operate on *public* trade information.

³The process of serving a market with the possibility to purchase and sell an asset.

compete over victim transactions, we perform simulations to quantify the transaction fees resulting from a reactive fee counter-bidding contest.

Summary of contributions:

- **Formalization of sandwich attacks.** We state a mathematical formalization of the AMM mechanism and the sandwich attack, providing an adversary with a framework to manage their portfolio of assets and maximize the profitability of the attack.
- **Analytic and empirical evaluation.** We analytically and empirically evaluate sandwich attacks on AMM DEX. Besides an adversarial liquidity taker, we introduce a new class of sandwich attacks performed by an adversarial liquidity provider. We quantify the optimal adversarial revenue and validate our results on the Uniswap exchange (largest DEX, with 5M USD trading volume at the time of writing). Our empirical results show that an adversary can achieve an average daily revenue of 3,414 USD⁴. Even without collusion with a miner, we find that, in the absence of other adversaries, the likelihood to position a transaction *before* or *after* another transaction within a blockchain block is at least 79%, using a transaction fee payment strategy of ± 1 Wei⁵.
- **Multiple Attacker Game.** We simulate the sandwich attacks under multiple simultaneous attackers that follow a reactive counter-bidding strategy [21]. We find that the presence of 2, 5 and 10 attackers respectively reduce the expected profitability for each attacker by 51.0%, 81.4% and 91.5% to 0.45, 0.17, 0.08 ETH (67, 25, 12 USD), given a victim that transacts 20 ETH to DAI on Uniswap with a transaction pending on the P2P layer for 10 seconds before being mined. If the blockchain is congested (i.e. the victim transaction remains pending for longer than the average block interval), we show that the break-even of the attacker becomes harder to attain.
- **DEX security vs. scalability tradeoff.** Our work uncovers an inherent tension between the security and scalability of an AMM DEX. If the DEX is used securely (i.e. under a low or zero price slippage), trades are likely to fail under high transaction volume; and an adversarial trader may profit otherwise.

II. DECENTRALIZED EXCHANGES

At the root of decentralized exchanges are blockchains. Blockchains, such as Bitcoin [48], enable peers to transact without trusting third-party intermediaries. The core component of a blockchain is a hash-linked chain of blocks [15], where miners form blocks as a data-structure which accumulates transactions. Blockchains which allow the execution of smart contracts [53], constitutes the basic building block for exchanges. A crucial aspect of this paper is

⁴We disclosed our preliminary results to Uniswap on 18th of November 2019, which allowed tightening the trader protections.

⁵The smallest amount of Ether currency, 1 WEI = 10^{-18} ETH

that in most blockchain designs, transactions are executed in the sequence in which they are written into a block. This sequence dependence matters for blockchain-based exchanges, and will be detailed extensively in Section III. An exchange is built out of three main components: a price discovery mechanism, a trade matching engine, and a trade clearing system. Blockchains allow these components to be encoded within a smart contract to construct a decentralized, or non-custodial exchange [33], [52], [5], [43], [39], [23]. The non-custodial property guarantees that a trader retains custody over their assets at any point in time. If all exchange components are implemented within smart contracts, the exchange qualifies as an *on-chain DEX*. If only the trade clearing is realized within a smart contract, the exchange may be centralized but can retain the non-custodial property [39].

A. DEX components

A DEX is a game between a liquidity provider and taker.

Liquidity Provider: a market participant that provides liquidity (financial asset trade offers).

Liquidity Taker: a market participant that buys or sells one asset in exchange for another asset, by taking the liquidity offered by a liquidity provider.

Further, we distinguish between two varieties of DEX, depending on their mechanisms of price discovery.

Order Book: a list of buy and sell orders for a particular asset, where each order stipulates a price and quantity. A liquidity provider quotes bid and ask prices, with an associated volume, competing for liquidity taker order flow [5], [43], [39], such that a match between supply (from a liquidity provider) and demand (from a liquidity taker) is facilitated (also referred to as *market making*).

Automated Market Maker (AMM): A predefined pricing algorithm automatically performs price-discovery and market making, using assets within liquidity pools [52], [4]. Liquidity providers are, therefore, not required to monitor the market to adjust bid and ask prices. Liquidity takers can directly trade against the AMM liquidity. Such automation also serves to reduce the number of on-chain transactions, making such mechanisms particularly suitable for smart contract-based DEXs given an underlying blockchain that supports only a limited number of transactions per second (tps).

B. AMM Mechanism

We denote with X/Y an asset pair composed of asset X and Y . An AMM asset pair X/Y consists of two liquidity pools, respectively for each asset:

Asset X liquidity pool ($x \in \mathbb{R}^+$): Total amount of asset X deposited by liquidity providers.

Asset Y liquidity pool ($y \in \mathbb{R}^+$): Total amount of asset Y deposited by liquidity providers.

Definition 1. The state (or depth) of an AMM market X/Y is defined as (x, y) , x the amount of asset X , y the amount of asset Y in the liquidity pool. The state at a given blockchain block N is denoted (x_N, y_N) .

AMM DEXs support the following actions.

AddLiquidity: A liquidity provider deposits δ_x of asset X , and δ_y of asset Y into the corresponding liquidity pools (cf. Equation 1).

$$(x, y) \xrightarrow[\delta_x \in \mathbb{R}^+, \delta_y \in \mathbb{R}^+]{\text{AddLiquidity}(\delta_x, \delta_y)} (x + \delta_x, y + \delta_y) \quad (1)$$

RemoveLiquidity: A liquidity provider withdraws δ_x of asset X , and δ_y of asset Y from the corresponding liquidity pools (cf. Equation 2).

$$(x, y) \xrightarrow[\delta_x \in \mathbb{R}^+ \leq x, \delta_y \in \mathbb{R}^+ \leq y]{\text{RemoveLiquidity}(\delta_x, \delta_y)} (x - \delta_x, y - \delta_y) \quad (2)$$

TransactXforY: A liquidity taker can trade δ_x of asset X , increasing the available liquidity of asset X , in exchange for $\delta_y = f(\delta_x - c_x(\cdot)) - c_y(\cdot)$ of asset Y , decreasing the available liquidity of asset Y (cf. Equation 3). $c_x(\cdot), c_y(\cdot)$ represent the trade fees in asset X and Y respectively. $f(\cdot)$ calculates the amount of asset Y purchased by the liquidity taker. Each AMM exchange may chose a custom pricing function $f(\cdot)$ for governing the asset exchange [1]. Note that the exchange asset pricing cannot be determined by a simple constant, as the market dynamics of purchasing and selling power must be modeled within the exchange (i.e. the more assets one would want to purchase, the higher the fees).

$$(x, y) \xrightarrow[\delta_x \in \mathbb{R}^+]{\text{TransactXforY}(\delta_x)} (x + \delta_x, y - f(\delta_x - c_x(\cdot)) + c_y(\cdot)) \quad (3)$$

Constant Product AMM. The simplest AMM mechanism is a constant product market maker, which keeps the product $x \times y$ constant for any arbitrary asset pair (X/Y). In this work we focus on the constant product model, because with over 75% market liquidity, this represents the most prevalent AMM model. In the following, k denotes the product of supplies ($k \in \mathbb{R}^+ = x \times y$), which remains constant upon taker transactions. k changes when a liquidity provider deposits, or withdraws X/Y pool funds. Equation 4 shows the state changes of **TransactXforY** under a constant product AMM.

$$(x, y) \xrightarrow[\delta_x \in \mathbb{R}^+]{\text{TransactXforY}(\delta_x)} (x + \delta_x, \frac{xy}{x + \delta_x - c_x(\cdot)} + c_y(\cdot)) \quad (4)$$

C. Price Slippage

Price slippage is the change in the price of an asset during a trade. *Expected price slippage* is the expected increase or decrease in price based on the volume to be traded and the available liquidity [51], where the expectation is formed at the beginning of the trade. The

higher the quantity to be traded, the greater the expected slippage (cf. Table I). *Unexpected price slippage* refers to any additional increase or decrease in price, over and above the expected slippage, during the intervening period from the submission of a trade commitment to its execution. This can be thought of as an expectation error. When an exchange's market liquidity changes, the resulting *actual* slippage is challenging to foresee (cf. Figure 1), making the formation of accurate expectations more challenging. We note the following definitions.

Expected Execution Price ($\mathbb{E}[P]$): When a liquidity taker issues a trade on X/Y , the taker wishes to execute the trade with the expected execution price $\mathbb{E}[P]$ (based on the AMM algorithm and X/Y state), given the expected slippage.

Execution Price (P): During the time difference between a liquidity taker issuing a transaction, and the transaction being executed (e.g. mined in a block), the state of the AMM market X/Y may change. This state change may induce unexpected slippage resulting in an execution price $P \neq \mathbb{E}[P]$.

Unexpected Price Slippage ($P - \mathbb{E}[P]$): is the difference between P and $\mathbb{E}[P]$.

Unexpected Slippage Rate ($\frac{P - \mathbb{E}[P]}{\mathbb{E}[P]}$): is the unexpected slippage over the expected price.

a) *Slippage Example:* For example, a liquidity taker, who intends to trade 1 asset X for 20 Y at an exchange, results in a price of 0.05, quoted in units of asset Y . However, by the time the AMM DEX executes this transaction, if the price increases to 0.1, the liquidity taker would only receive 10 Y for 1 X . The unexpected slippage, in this case, is $0.1 - 0.05 = 0.05$. Slippage can also be negative, i.e. a liquidity taker can receive more asset Y than expected. If the execution price above decreases to 0.25, the liquidity taker would receive 40 Y for 1 X , with a corresponding unexpected slippage of $0.1 - 0.25 = -0.15$.

III. SANDWICH ATTACKS ON AMM DEXES

In traditional financial markets, the predatory trading strategy of *front-running* involves exploiting (typically non-public) information about a pending trade, expected to materially change the price of an asset, by buying or selling the asset beforehand [6]. If the asset is expected to rise (fall) in price as a result of the trade, the front-

	AMM State 1		AMM State 2	
Liquidity X (x)	100		1,000	
Liquidity Y (y)	10		100	
Product ($k = xy$)	1,000		100,000	
Purchase amount X	1	10	1	10
AMM Price Y/X	0.1000	0.1000	0.1000	0.1000
$\mathbb{E}[P] Y/X$	0.1010	0.1111	0.1001	0.1010
Expected slippage	0.0010	0.0111	0.0001	0.0010
Slippage rate	1.01%	11.11%	0.10%	1.01%

TABLE I: Example price slippages on an AMM DEX.

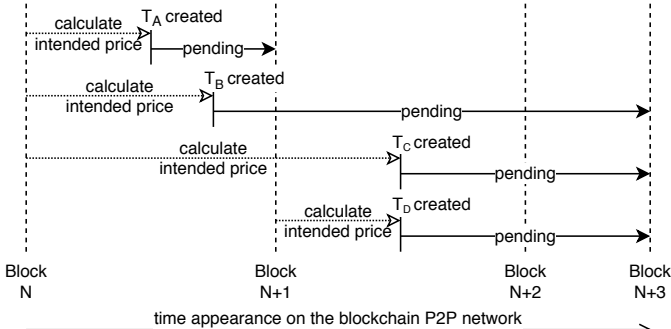


Fig. 1: Visualizing the cause of unexpected slippage. $\mathbb{E}[P]$ of T_A is based on the AMM state of block N . T_A does not suffer from unexpected slippage, because no concurrent transactions exist. T_B executes in block $N + 3$. $\mathbb{E}[P]$ of T_C 's is based on block N , as we assume network delays. If T_C and T_D change the state of the underlying market, those may induce unexpected slippage for T_B .

runner will seek to buy (sell) the asset before the large pending transaction executes. AMM DEXs aim to mitigate malpractice by providing complete transparency about the available liquidity for assets X, Y , all pending and performed trades, and therefore removing the role played by non-public information. However, AMM DEXs also exacerbate malpractices by quoting asset prices in a fully deterministic way, providing relative certainty over the expected price impact of a trade. This enables a front-running adversary to perform attacks with predictable outcomes. In the following, we study two sandwich attacks on constant product AMM asset exchanges:

- 1) Liquidity taker attacks liquidity taker.
- 2) Liquidity provider attacks liquidity taker.

In each case, the fundamental intuition is that the delay in the time taken for a transaction to execute allows an adversary to profit by exploiting the knowledge of the direction of a price change. The attacks are called sandwich attacks because a victim transaction is *sandwiched* between adversarial transactions.

A. System Model

We consider a blockchain P2P network, where a victim initiates trades on an AMM DEX (cf. Figure 2). An adversary observes pending victim transactions (i.e. not yet mined transactions within the memory-, or mempool) through a spy node (e.g. a custom Ethereum client), and a miner chooses to include transactions within a block according to a policy (cf. Section VI). A victim transaction trades a crypto-currency asset (such as ETH, DAI, SAI, VERI) to another crypto-asset. We do not consider blockchain forks. While blockchains typically provide delayed finality after k blocks [27], [29], we consider a transaction final once included within a block.

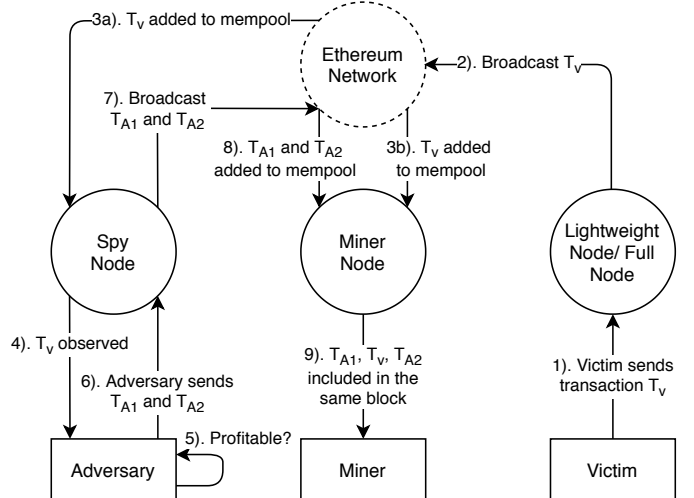


Fig. 2: Sandwich attack system.

B. Threat Model

We consider one computationally bounded and economically rational adversary A (cf. Section VII for an extended threat model with multiple adversaries), that observes a zero-confirmation transaction T_V from a victim trader V on a blockchain P2P network. The adversarial trader can issue its own transaction $T_{A,f}$ with a transaction fee f . Depending on f , and the age of propagation, $T_{A,f}$ may be included within the blockchain prior or past T_V (cf. Section VI). In this work we focus on these novel cases where the adversary is not colluding with a miner, i.e. we weaken the adversary to quantify a lower bound on the feasibility and profitability of the proposed attacks. Outside of this work, a (stronger) adversary may collude, or bribe a miner [40], [46], [14], to influence the transactions ordering within a block, or even to fork the chain as in to discard unsuccessful attacks. We moreover assume that an attack against one victim transaction is independent from other concurrent attacks towards other victim transactions.

C. Liquidity Taker Attacks Taker

In our first attack, a liquidity taker targets a victim liquidity taker who has emits on the blockchain P2P network an AMM DEX transaction (`TransactXforY`), formalizing [4]. The adversary then emits two transactions (one front- and one back-running) to exploit the victim transaction T_V (cf. Figure 3). These three transactions are then unconfirmed in the blockchain P2P network, until a miner chooses to include and execute them within a block. The adversary can influence the position of the adversarial transactions, relative to the victim transaction, by paying a higher, or lower transaction fee amount (cf. Section VI).

We refer the interested reader to the Appendix A-A for the technical details of the involved transactions.

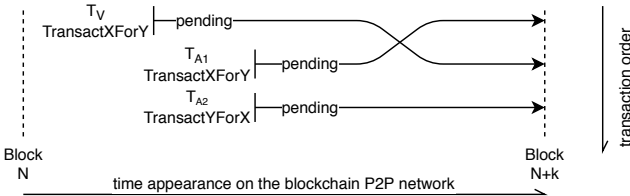


Fig. 3: An adversarial liquidity taker A attacks a victim taker V on an AMM DEX. Transaction T_V specifies its slippage protection based on the AMM state of block N . The adversary's goal is to include T_{A1} , T_V and T_{A2} in the same block $N + k$, $k \in \mathbb{Z}^+$ in that sequence.

D. Liquidity Provider Attacks Taker

We present a novel sandwich attack where a liquidity *provider* targets a victim liquidity taker transaction (`TransactXforY`) on the blockchain P2P network. Upon observing the victim transaction, the adversary emits three transactions (cf. Figure 4):

- 1) `RemoveLiquidity` (increases victim's slippage)
- 2) `AddLiquidity` (restores pool liquidity)
- 3) `TransactYforX` (restores asset balance of X)

The (i) front-running `RemoveLiquidity` transaction reduces the market liquidity of the AMM DEX and increases the victim's unexpected slippage. The (ii) back-running `AddLiquidity` transaction restores the percentage of liquidity A holds before the attack. Finally, (iii) the back-running transaction `TransactYforX` equilibrates the adversary's balance of asset X to the state before the attack.

Note that liquidity providers earn commission fees proportional to the liquidity (i.e. the amount of assets) they provide to an AMM DEX market. In this attack, the adversary A withdraws all its assets from the liquidity pool before T_V executes. As such, A foregoes the commission fees for the victim's transaction. We refer the interested readers to Appendix A-B for further technical details.

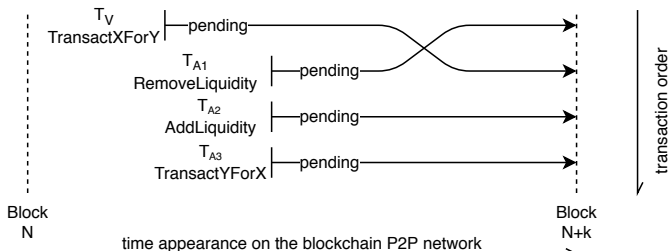


Fig. 4: An adversarial liquidity provider A attacks a victim taker V . T_V transacts asset Y for asset X .

E. Model Limitations

1) *Margin and Leveraged Trading:* Margin trading is the process of using borrowed funds to amplify trading profits (or losses). A trader commits a percentage of the total trade value to open a margin position. For example,

to open a $5 \times$ short ETH for DAI position with 10ETH, the trader needs to commit 2ETH as collateral. A short position reflects the expectation that the ETH price will decrease, whereas a long position reflects the opposite. The margin platform will then lend to the trader 10ETH and convert those assets to DAI. If the ETH price decreases, the trader can close the margin trade with a profit.

A limitation of our work is that we do not consider on-chain margin platforms utilizing AMM exchanges to open short/long positions (e.g. the recently attacked bZx platform [49]). An on-chain margin trade system would enable an adversary to reduce the capital requirements for sandwich attacks, at the cost of higher transaction fees (for opening and closing margin trades). Margin trading is unlikely to affect the adversary's monetary revenue because the victim configures a fixed slippage.

2) *Blockchain Forks:* We do not consider the impact of stale blocks in our analysis. In practice, it is possible that a transaction is included in a stale block (on the forked chain), but is not included in the confirmed blocks (on the main chain). This stale transaction is typically re-injected into the blockchain client's mempool when the stale block is added as an uncle to the main chain. The stale re-injection process of adversarial and victim transaction may increase the failure rate of sandwich attacks, but we leave quantitative results for future work.

IV. ANALYTICAL EVALUATION

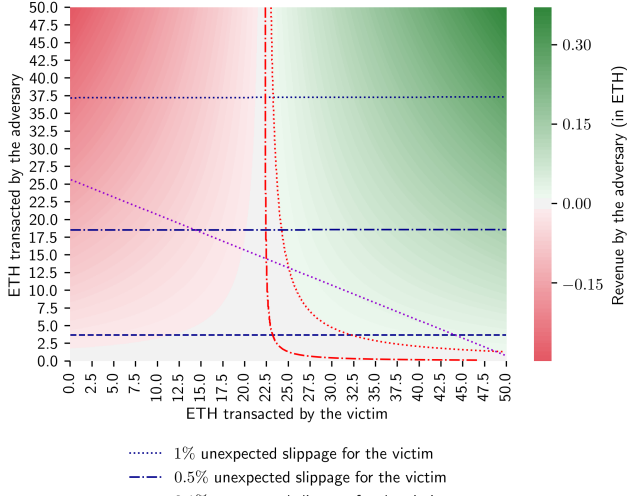
In this section, we perform the analytical evaluation of sandwich attacks on Uniswap [52]. Uniswap is the most popular DEX at the time of writing with 1,301 markets, on average 7.30 provider per market and 29.3M USD liquidity. From Uniswap's inception in November 2018 to November 2019, we identified a trade volume of 1.6M ETH (248M USD), measured on a full archive Geth node (6-core Intel i7-8700 CPU, 3.20GHz, 64GB RAM, 10TB SSD)⁶. In what follows, we base our evaluations on Uniswap parameters and adopt its liquidity pool distributions [52] from Ethereum block 9M (mined 25th November 2019). In this section we present the analytical results for the two sandwich attacks presented in Section III-C and III-D.

A. Adversarial Liquidity Taker

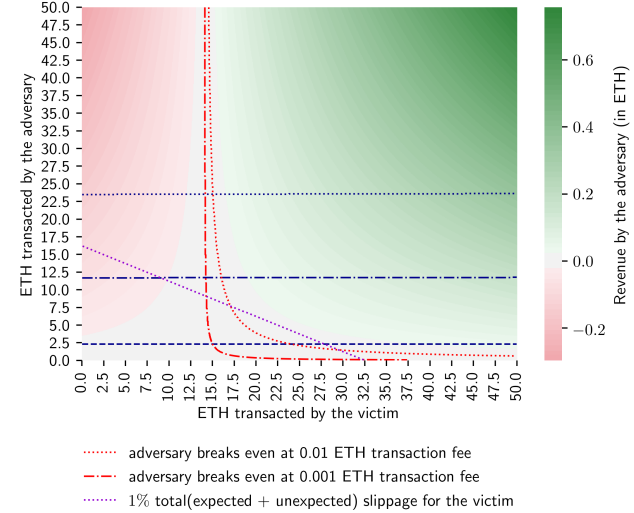
At Ethereum mainnet block 9M, the ETH/SAI Uniswap offers 7,377.53 ETH and 521,468.62 SAI⁷. The ETH/DAI Uniswap offers 4,660.75 ETH and 693,706.47 DAI. Given this market information, and the constant product formula (cf. Section II), we plot in Figure 5(a) and 5(b) the revenue of an adversarial taker performing a sandwich attack against another taker. We visualize three unexpected slippage thresholds (0.1%, 0.5% and 1%). We plot the lines at which an adversary would break even given a total

⁶We focus only on transactions executed on Uniswap endpoints directly, not internal transactions that are routed to Uniswap.

⁷In the following we adopt the ETH/SAI exchange rate at block 9M as the ETH/USD exchange rate. 1 ETH = 148.97 USD



(a) ETH/SAI market



(b) ETH/DAI market

Fig. 5: Analytical sandwich attack by a liquidity taker on a taker (Uniswap, block 9M, 0.3% fees, 0.5% unexpected slippage). If T_V transacts 40 ETH for SAI, A gets a max. revenue by front-running T_V with a trade 18.59 ETH for 2,754.32 SAI, and back-running with 2,754.32 SAI for 18.68 ETH. This results in a profit of 0.08 ETH (11.74 USD), if A bears 0.01 ETH tx fees. Note that the two sub-legends of each figure apply to both sub-figure 5(a) and 5(b).

(T_{A1} and T_{A2}) of 0.01 ETH (1.97 USD) and 0.001 ETH (0.2 USD) worth of transaction fees⁸. We observe that the greater the amount of ETH transacted by the victim, the greater is the adversarial revenue. For example, given an unexpected slippage protection of 0.5%, an adversarial taker gains a revenue of 0.01 ETH (2.03 USD) for a victim transaction trading 25 ETH to SAI on Uniswap. In contrast, the adversary gains a revenue of 0.14 ETH (20.71 USD), if the victim trades 50 ETH instead of 25.

a) *Optimal Adversarial Revenue*: Out of the over 1,300 Uniswap exchange markets (i.e. coin pairs to trade) an adversary may need to focus and hold liquidity in selected markets. In Figure 6 we quantify the maximum revenue an adversary can expect in a given market, conditional on a suitable victim transaction. Note that MKR has the highest liquidity (9,759.83 ETH and 2,830.27 MKR), followed by SAI (7,377.53 ETH and 1,099,040.91 SAI), WETH (5,642.08 ETH and 5,632.25 WETH), SNX (5,262.53 ETH and 572,512.14 SNX) and DAI (4,660.75 ETH and 693,706.47 DAI).

b) *Minimum Profitable Victim Input*: Not every victim transaction yields a profitable attack. For each of the five exchanges in Figure 6, we quantify a minimum profitable victim input \min_{input} (under 0.01 ETH transaction fee and 0.3% commission), under which an adversary will be unable to make a profit (e.g. 24.26 ETH for SAI per Figure 6). This minimum profitable victim input amount increases with the liquidity pool size

⁸At the time of writing, the average Ethereum transaction fee is 0.13 USD (<https://bitinfocharts.com/comparison/ethereum-transactionfees.html>)

(cf. Figure 7). The adversary's optimal input increases only slightly (cf. the near horizontal line on Figure 6) with the victim transaction size, because the ETH value transacted by the victim is relatively small compared to the total amount of ETH in the Uniswap exchange. Given a fixed total slippage, we observe that markets with higher liquidity (e.g. SAI, MKR) yield higher potential revenues than lower-liquidity markets (e.g. SNX and DAI) (given the appropriate victim transaction).

B. Adversarial Liquidity Provider

Figure 8(a) and 8(b) show the revenue of an adversarial liquidity provider (cf. Section III-D), after T_V . We visualize the same adversarial break even lines at 0.01 ETH (1.97 USD) and 0.001 ETH (0.2 USD). Note that the adversary can only withdraw a limited amount of liquidity without triggering the slippage protection on victim's transaction. By removing liquidity from an AMM market, the liquidity provider is forgoing a market commission (0.3% for Uniswap). To gauge profitability, we consider the following example where T_V purchases 100 ETH from the SAI Uniswap exchange with 0.5% unexpected slippage. The optimal strategy is to withdraw 26.58% of the total liquidity pool, which leads to a revenue of up to 0.28 ETH (41.71 USD) for the adversary. A passive liquidity provider with 26.58% of the liquidity pool would only earn 0.08 ETH (11.91 USD) given a commission of 0.3%.

a) *Who Loses Money?*: Both V and other honest liquidity providers lose money. V purchases 100 ETH with 15,223.02 SAI without triggering a 0.5% slippage protection as a result of A 's front-running transaction.

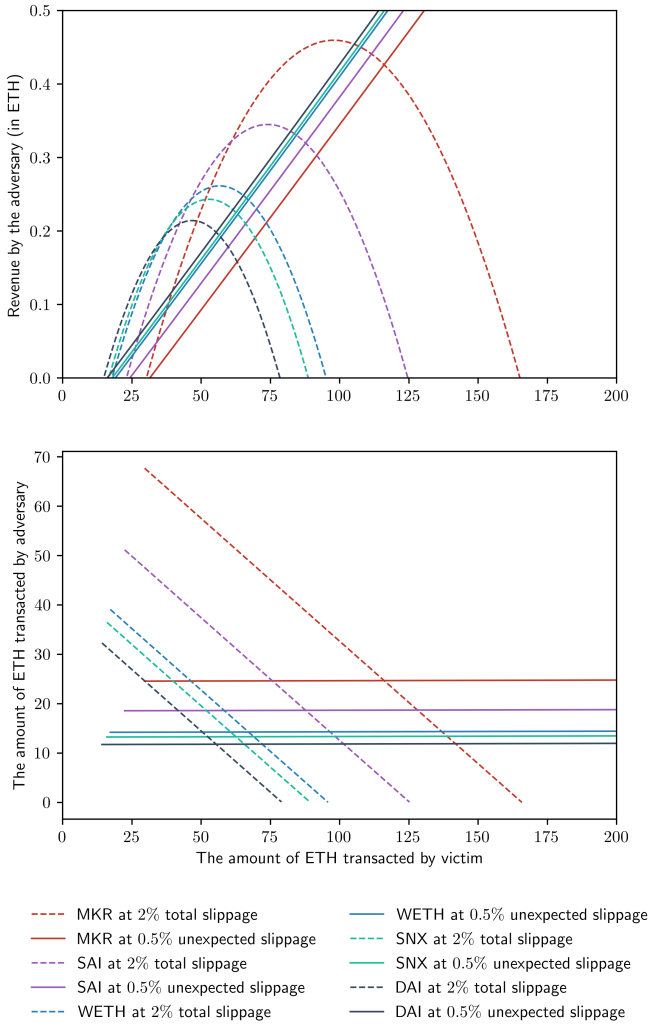


Fig. 6: Sandwich attack optimal revenue for an adversarial taker when V trades on five Uniswap markets (0.3% fee, A breaks even at 0.01 ETH).

With no adversary, V only needs 15,147.28 SAI for the same amount of ETH, which is 75.74 SAI less. In addition, this V transaction should increase the liquidity pool from (7,377.53 ETH / 1,099,040.91 SAI) to (7,277.53 ETH / 1,114,263.92 SAI). Post attack, the liquidity pool remains with 7,277.25 ETH and 1,114,263.92 SAI, i.e. A gains $7,277.53 - 7,277.25 = 0.28$ ETH from the liquidity pool.

b) Optimal Adversarial Revenue: We quantify the optimal adversarial revenue in Figure 13, *after subtracting the foregone opportunity cost* (e.g. 0.3% for liquidity provider on Uniswap), conditional on a suitable victim transaction. We observe that the forgone commission fee is relatively stable, given a fixed total slippage, because the adversary must satisfy the victim's slippage limit. We also quantify in Figure 9 the minimum victim input.

c) Impact of Coin Decimals: The number of decimal places for ERC20 tokens is configurable, though most of

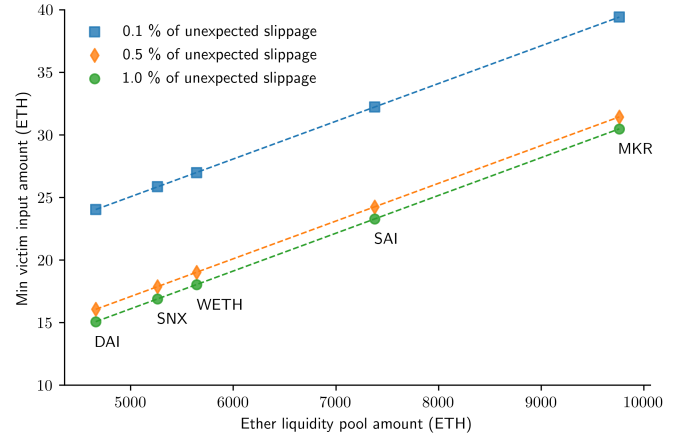


Fig. 7: Minimum profitable victim input on five Uniswap markets (0.3% fee, A breaks even at 0.01 ETH, 0.5% unexpected slippage). A liquidity taker does not yield a profit if T_V trades less than 24.26 ETH for SAI.

the coins have 18 decimal places. For example, USDC, which is the 7th largest Uniswap exchange at block 9M, has 6 decimal places behind the comma. In Figure 9, we plot the $k = xy$ curve for SAI if it had 17 decimal places instead of 18. The minimum victim transaction amount for A increases from 43.93 ETH to 44.54 ETH, if the victim purchases ETH using SAI. The minimum victim transaction amount also increases from 45.3 ETH to 56.3 ETH for ETH to SAI transactions.

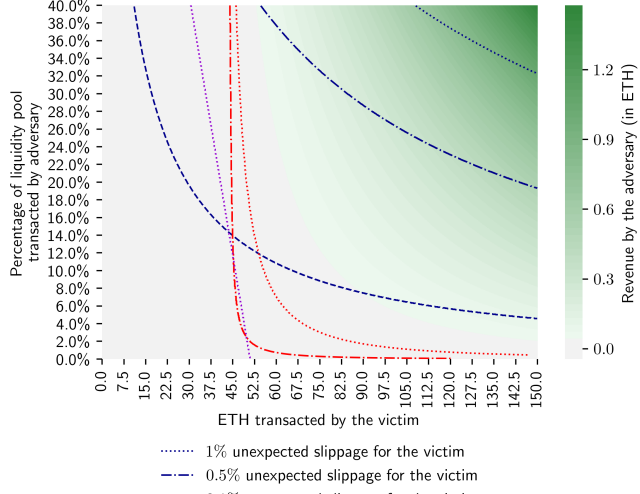
C. Overall success of the attacks

Overall, when analytically evaluated, both an adversarial liquidity taker and provider can profit by undertaking a sandwich attack. The optimal adversarial revenue, however, depends on the slippage protection setting. By fixing the unexpected slippage, the adversary's revenue increases linearly against the amount of ETH transacted for both adversarial takers and providers. Alternatively, fixing the total slippage (unexpected + expected slippage) would yield an upper bound for both the victim transaction size and adversarial optimal profit.

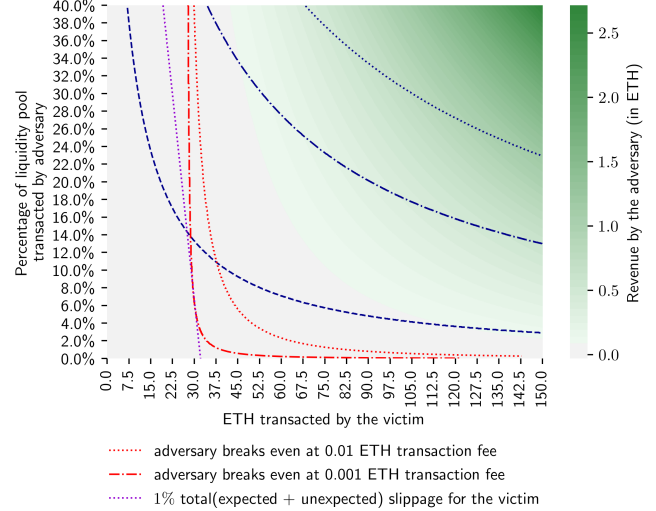
V. EMPIRICAL EVALUATION

Our experimental setup corresponds to the system model in Figure 2, with a modified adversarial Parity client. We increase the maximum number of transactions in the pool of unconfirmed transactions (mempool) from the default 1024 to 2048. We design a Python script that subscribes to the modified pub/sub functionality of Parity and listens for new pending transactions of the target Uniswap market. Our script computes the profitability of any given victim transaction, and if an adversarial strategy proves profitable, the script generates and propagates the corresponding front- and back-running transaction.

We conduct both experiments (cf. Section V-A and V-B) on the main Ethereum network against the ETH/VERI



(a) ETH/SAI market



(b) ETH/DAI market

Fig. 8: Sandwich attack by a liquidity provider on a taker (Uniswap, block 9M, 0.3% fees). If T_V trades SAI for 60 ETH with an unexpected slippage of 0.5%, A can achieve a max. revenue by front-running T_V with removing 37.76% of liquidity (eq. 2, 785.97 ETH and 415,030.47 SAI), and regain 37.76% of liquidity (deposit 2,749.57 ETH and 420,542.21 SAI) by back-running T_V . Upon rebalancing to ETH, A gains a profit of 0.07 ETH (10.55 USD, break-even 0.01 ETH).

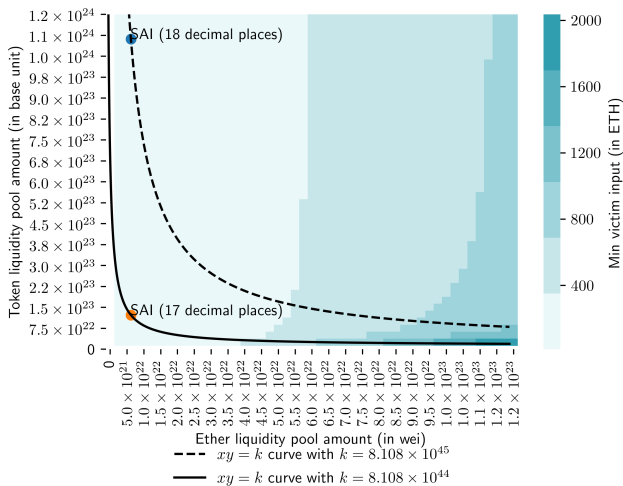


Fig. 9: Minimum profitable victim input on SAI Uniswap market (0.3% fee, 0.5% unexpected slippage, adversary break even at 0.01 ETH tx fees). A cannot gain any profit, if T_V trades SAI for less than 43.93 ETH. If SAI had 17 decimal places after the comma instead of 18, the min. victim transaction amount increases to 44.54 ETH.

Uniswap market and only attack our transactions. The ETH/VERI market offers the smallest liquidity (0.01 ETH and 0.07 VERI, total 3.50 USD) out of the 78 Uniswap exchanges on the Uniswap UI as of block 9M. To ensure that our results are sufficiently representative, we consider a time window of 158 days, i.e. several months. Our

adversarial node runs on AWS in Ireland, (4 vCPU, AMD EPYC 7000, 2.5 GHz, NVMe SSD, max. 10 Gbps network). The experiments result in three outcomes: (i) success (all adversarial transactions are included in the same block as T_V), (ii) the front- and back-running transactions are successful, but not all adversarial transactions are included in the same block as T_V , and (iii) front- or/and back-running failed.

a) *Computing the adversarial transactions:* Three steps allow us to compute the optimal adversarial input amount. First, the maximum amount A can transact without breaking V 's slippage protection (denoted by \hat{o}) is computed using a binary search. Second, we calculate if the attack is profitable if A inputs \hat{o} . As Figure 3 and 4 suggest, if an attack is not profitable at \hat{o} , then it is not profitable for any $o < \hat{o}$. Finally, because Uniswap uses integer divisions, there might exist $o < \hat{o}$, which results in the same or more profit. We perform a ternary search to find the optimal input.

A. Liquidity Taker Attacking Taker

We issue and attack T_V purchasing VERI with 0.001 ETH. T_V is triggered through the Uniswap UI (default 0.5% unexpected slippage) and at the time of writing default Metamask gas price (5 GWei⁹). We repeat this attack 20 times, and report the results in Table II. On average, the adversary discovers T_V within 450ms, and requires less than 200ms to compute and send out T_{A1} and T_{A2} . During our experiment, T_V remains in the adversary's

⁹1 GWei = 1×10^{-9} ETH

mempool for an average of 35.84 seconds. We achieve a success rate of 19 out of 20 attempts. One experiment failed, where the victim’s transaction T_V remained in the adversarial’s mempool for only 1.677 seconds. In 8 out of 20 experiments, the attack is partially successful, because the back-running transaction T_{A2} is mined in a later block than T_V . Two possible causes are that either T_{A2} is received after T_{A1} and T_V are mined, or the block that mined T_V is full. We observe that the respective T_V are mostly positioned at the end of the block, which may indicate network congestion.

B. Liquidity Provider Attacking Taker

We initialize the adversary by adding liquidity to the ETH/VERI Uniswap contract. We again issue T_V purchasing VERI with 0.002 ETH via the Uniswap UI, Metamask (2 GWei), and attack with our adversarial node. We also repeat this attack 20 times. Table II shows a summary of our experiment results. Compared to Section V-A, T_V remains, on average less than 10 seconds in the mempool, which may indicate that the blockchain network is less congested at the time of the experiment. We also observe that the adversarial transactions are relatively closer to T_V within the block. We achieve a success rate of 20 out of 20 attempts.

	Adversarial Taker		Adversarial Provider	
	Mean	STD	Mean	STD
T_V Broadcast Duration	0.45s	0.27	0.36s	0.29
A Find Strategy Duration	0.03s	0.00	0.03s	0.00
A Execute Strategy Duration	0.16s	0.60	0.04s	0.00
T_V Duration In Mempool	35.84s	33.31	23.09s	10.52
T_{A1} Duration In Mempool	35.88s	33.19	23.03s	10.52
T_{A2} Duration In Mempool	48.87s	51.25	23.03s	10.52
T_{A3} Duration In Mempool	N/A	N/A	23.03s	10.52
A1 Block Relative Position	0.05	0.22	0.00	0.00
A1 Index Relative Position	-10.42	10.26	-2.95	2.34
A2 Block Relative Position	0.70	0.92	0.00	0.00
A2 Index Relative Position	5.45	6.47	4.50	4.90
A3 Block Relative Position	N/A	N/A	0.00	0.00
A3 Index Relative Position	N/A	N/A	5.50	4.90
Success	11/20		20/20	
Partial Success	8/20		0/20	
Failure	1/20		0/20	

TABLE II: Results for the liquidity taker/provider attacks taker. The victim’s transaction T_V was triggered manually using Metamask through Uniswap UI. Adversarial node and victim have a clock difference of $8.781ms \pm 6.189ms$.

1) *Foregone Adversarial Revenues:* To understand the financial potential of our attacks, we estimated the theoretical revenue for the 79 exchanges of the Uniswap UI between block 8M and 9M (i.e. recent blocks at the time of writing), assuming a break-even at 0.01 ETH transaction fees. Our results (cf. Table III) suggest that within the reported 158 days, an adversary could have achieved a revenue of 440,749.02 USD when attacking as a taker, and 98,666.15 USD when attacking as a liquidity provider. 7.4% of transactions are profitable when attacking as a taker, while 4.2% when attacking as a provider.

	Profitable TXs / Total TXs	Revenue (ETH)	Revenue (USD)
Liquidity taker attacks taker			
ETH → Token	878/25, 204	98.15	14,621.41
Token → ETH	5,657/602, 85	2,643.84	393,852.46
Token → Token	1,258/196, 72	216.66	32,275.16
Total	7,793/105, 161	2,958.64	440,749.02
Liquidity provider attacks taker			
ETH → Token	444/25, 204	52.55	7,829.05
Token → ETH	3,254/60, 285	520.61	77,555.62
Token → Token	721/19, 672	89.16	13,281.49
Total	4,419/105, 161	662.32	98,666.15

TABLE III: Estimated adversarial revenue for the 79 exchanges on the Uniswap UI, assuming an adversarial break even cost of 0.01 ETH. Data of 158 days considered (block 8M to 9M).

C. Slippage

To help an adversary understand how takers configure their slippage, we plot the estimated distribution of expected slippage and maximum allowed unexpected slippage in Figure 10. Note that we are using block N ’s state to calculate the slippages of a transaction mined at block $N+1$. Therefore, these slippages are only estimates, as we do not know the exact block state used by the taker to create transactions. Past Uniswap transactions have an average expected slippage of 0.58%, and an average unexpected slippage of 1.16%.

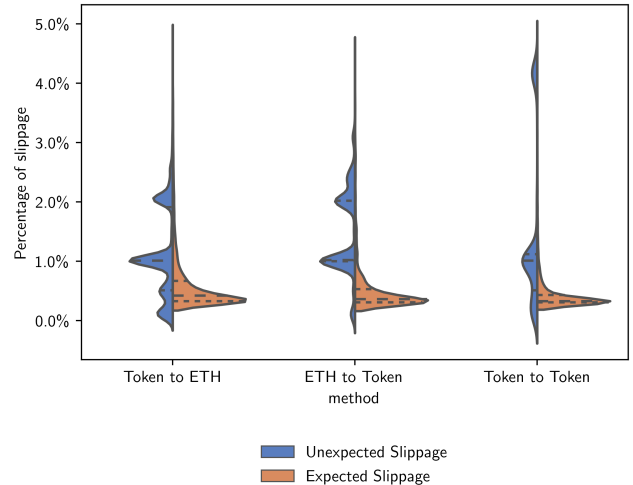


Fig. 10: Estimated expected and maximum permitted unexpected slippage on Uniswap transactions (block 8M to 9M). Most takers trade with c. 1% of maximum unexpected slippage (the Uniswap default at the time).

D. Overall success of the attacks

Our empirical results suggest that both an adversarial liquidity taker and provider can again profit by undertaking a sandwich attack, where the victim trades with the

Uniswap default slippage protection strategy at the time of writing this paper (0.5% total slippage). We crawled the previous transactions on Uniswap, where it shows that the most common unexpected slippage configuration is 1%, which is higher than the 0.5% default total slippage and therefore leads to higher front-running profit. Our experiments result in a high success rate (only 1 out of 40 failed), mainly because the Ethereum network was not congested, and the VERI market relatively inactive.

VI. HOW MINERS ORDER TRANSACTIONS

One crucial aspect of the potential profitability of the sandwich attacks centers on how miners order transactions within blocks. Blockchains typically prescribe specific rules for consensus, but there are only loose requirements for miners on how to order transactions within a block. To gain insight into this, we crawled the Ethereum blockchain from block 6,627,917 (where Uniswap was launched) to block 9M, constituting a total of 2,372,084 blocks, or equivalently 388 days of data. For each block, we classified the order of its transactions into one of four classes:

Empty: A block without transactions.

Gas Price: All transactions are sorted in descending order according to the gas price of each transaction.

Parity Default: Transactions are split into groups according to Parity’s prioritization (e.g. local transactions first, penalized transactions last). Then, within each group, the transactions are sorted in descending order according to each transaction’s gas price.

Unknown: Transactions are not ordered by the gas price and do not follow parity’s default strategy.

The treatment of transactions depends on the Ethereum client. At the time of writing, 78.3% of the Ethereum clients operate Geth, respectively 20.2% Parity¹⁰. Geth first sorts and separates the list of transactions into lists of individual sender accounts and sorts them by nonce. Afterward, they are merged back together and sorted by gas price, always comparing only the first transaction from each account. Parity, by default, prioritizes local and retracted transactions first, and polishes transactions with heavy computation, and then sorts by gas price. A transaction is considered local if it is received via the RPC interface, or the sender of the transaction is part of the list of locally managed accounts. Miners may choose to modify the transaction inclusion policy arbitrarily. To individually categorize each block, we first analyzed the gas price of each transaction and started by extracting the gas price only for the first transaction of each sender, while ignoring the other transactions from the same sender. We only consider the first transaction because a higher gas price transaction can be placed behind another transaction with a smaller nonce. If the extracted gas price list is sorted, we classify the block as following the “gas price” strategy. Alternatively, we verify if the gas price list consists of

multiple sublists of gas prices, where the gas prices within each sublist are sorted in descending order. Each sublist represents a priority group, where transactions within the same priority group are sorted by gas price. If there are no more than four sublists of gas prices (local, retracted, normal, penalized), we classify the block as a “Parity default” block, otherwise, as “unknown”.

Because both Parity and Geth sort transactions by default by gas price, it is difficult to identify which client a miner uses. Moreover, our heuristics may misclassify blocks as being ordered using gas price instead of Parity’s default strategy. A miner could have no local transactions for the block, and all transactions are thus ordered by gas price. The number of blocks classified as Parity default should, therefore, be regarded as a lower bound. We leave it for future work to develop a more precise client fingerprinting strategy.

A. Miner Transaction Ordering Results

Our results (cf. Table V and Table IV suggest that roughly 79% of the miners order transactions based on the gas price, thus likely following Geth’s strategy, and 16% order their transaction after Parity’s default strategy. These results are consistent with the client usage distribution. We find that 2% of the blocks are empty. 3% of the miners follow an unknown ordering method. We can conclude that to position a transaction *before* or *after* a target transaction, it is, with a probability of 79%, sufficient to pay a higher (+1 Wei) or lower gas price (-1 Wei) — assuming the absence of other front-running adversaries. If two transactions pay the same gas price, according to their source code, Parity and Geth include the transactions after the FIFO principle.

Overall, we find that most miners (c. 79%) order transactions based on the gas price. The dominance of this transaction order aids an adversary because it makes it more likely for an adversary that they can control the placement of their transactions in a block by tweaking the gas price they offer for each transaction.

B. Gas Price Distribution

We investigate the gas prices for each transaction over 189,951,899 transactions included in blocks 6,627,917 until block 9M (388 days of data). A gas price of 0 ETH might indicate that the transaction belonged to the miner. We find that a transaction has an average gas price of 17.2 ± 10520.1 GWei. The median gas price is 10 Gwei and the most frequently used gas price is 20 Gwei with 23,759,990 transactions (12.5%).

VII. MULTIPLE ADVERSARIES

Our prior analysis only considers the case of a single adversary. In this section, we analyze the possible implications of multiple attackers on the feasibility and profitability of sandwich attacks through simulations.

¹⁰<https://www.ethernodes.org/>

Miner Address	Transaction Ordering Strategy					Total Blocks
	Empty	Gas Price	Parity Default	Unknown		
0xea674fddc714fd979de3edf0f56aa9716b898ec8	9,434	400,546	171,428	23,254	604,662	
0x5a0b54d5dc17e0adc383d2db43b0a0d3e029c4c	16,329	423,103	93,903	35,348	568,683	
0x829bd824b016326a401d083b33d092293333a830	7,727	275,013	1,900	20	284,660	
0x52bc44d5378309ee2abf1539bf71de1b7d7be3b5	259	210,061	59,141	369	269,830	
0xb2930b35844a230f00e51431acae96fe543a0347	0	110,079	19,271	125	129,475	
0x04668ec2f57cc15c381b461b9fedab5d451c8f7f	7,130	42,405	257	0	49,792	
0x2a65aca4d5fc5b5c859090a6c34d164135398226	1,021	25,569	10,892	251	37,733	
0x2a5994b501e6a560e727b6c2de5d856396aadd38	1,170	31,543	5	0	32,718	
0x005e288d713a5fb3d7c9cf1b43810a98688c7223	1,097	27,926	30	0	29,053	
0x35f61dfb08ada13eba64bf156b80df3d5b3a738d	435	28,214	68	0	28,717	

TABLE IV: Classification of the top 10 miners in Ethereum, in terms of the number of blocks mined between blocks 6,627,917 until 9M (388 days). We see that miners seem to switch among strategies. Moreover, 4 out of the ten miners always seem to follow a known strategy. They either order their transactions by gas price or by using Parity’s default strategy. We also note that the address 0xb293..0347 is the sole miner who did not mine any empty blocks.

Strategy	Number of Blocks	Ratio
Empty Block	55,545	0.0234
Order per Gas Price	1,862,800	0.7853
Order per Parity Default	384,150	0.1620
Unknown Ordering	69,589	0.0293
Total	2,372,084	1.0000

TABLE V: Miner transaction ordering methodology between blocks 6,627,917 and 9M (388 days).

A. Extended Threat Model

We extend our threat model from Section III, to account for additional attackers. For simplicity, we assume that all adversaries have access to the same financial resources, internet connection, latency, and computational power. We identify the following key parameters that impact the outcome of the simulated game:

Number of Attackers: Intuitively, the more adversaries are attacking a victim transaction T_V , the harder this endeavor becomes for each attacker. In the following, we consider 2, 5, and 10 adversaries, which simultaneously attack a T_V .

Attacker Strategy: Previous work [21] suggests two transaction fee bidding strategies, namely an adaptive (reactive counter-bidding) and a non-adaptive (blind raising) adversarial strategy. We assume that all adversaries follow the reactive counter-bidding strategy, i.e. an adversary emits a higher transaction fee bid once the adversary observes a competing transaction. This strategy is not necessarily optimal, but it may estimate a lower bound for the sandwich attack’s front-running transaction cost.

We assume all adversaries are rational and attack with the parameters determined by the strategy from Section V, i.e. each adversary attempts to maximize its profit by fully exploiting the victim transaction’s allowed slippage.

For a two-player game, we show in Table VI, the possible transaction permutations after the adversarial transactions are mined. We show that the adversary who

manages to execute the first front-running transaction successfully “wins” the sandwich attack. This is because the victim transaction fails if both A and O execute the sandwich attack. If the other adversary is irrational and insists to execute the attack (by e.g. disregarding slippage protections), both adversaries lose, because both adversarial front-running transactions fail (e.g. $T_{A1} \checkmark, T_{O1} \times, T_V \times, T_{O2} \checkmark, T_{A2} \checkmark$).

B. Extended System Model

a) *Network Layer:* The speed at which an adversarial transaction propagates within the blockchain P2P network influences the number of reactive counter-bids it receives and the time the transaction is mined. Related works have extensively studied the asynchronous nature of blockchain P2P propagation [24], [22], [29], [28]. The propagation is affected by several factors, such as the network topology, number of nodes, internet latency, bandwidth, and network congestion, etc. In our work, we assume that the adversary directly establishes a point-to-point connection with the miner and the victim. Our study thereby abstracts away the number of nodes in the network, the network topology, intermediate devices (replay nodes, routes, and switches) and TCP congestion control. Equation 5 shows how we approximate transaction propagation duration.

$$\text{Propagation Duration} = \frac{\text{Transaction Size}}{\text{Bandwidth}} + \text{Latency} \quad (5)$$

To determine the distribution of transaction sizes, we crawl raw transactions sent to the Uniswap DAI market over 100,000 consecutive blocks, starting from block 9M. Our measurements suggest a mean transaction size of 426.27 ± 68.94 Bytes, which we use as parameters for an assumed normal distribution of the adversarial and victims’ transaction sizes. For the latency and bandwidth distribution, we take the mean percentile statistics [37], [28] and apply linear interpolation to estimate the underlying cumulative probability distribution (cf. Table VII).

Transaction Execution Order (left to right)					Winner	Reward for Attacker <i>A</i>	Reward for Attacker <i>O</i>
$T_{A1} \checkmark$	$T_{O1} \times$	$T_V \checkmark$	$T_{O2} \times$	$T_{A2} \checkmark$	<i>A</i>	Revenue – Fee(T_{A1}) – Fee(T_{A2})	–Fee(T_{O1}) – Fee(T_{O2})
$T_{A1} \checkmark$	$T_{O1} \times$	$T_V \checkmark$	$T_{A2} \checkmark$	$T_{O2} \times$	<i>A</i>	Revenue – Fee(T_{A1}) – Fee(T_{A2})	–Fee(T_{O1}) – Fee(T_{O2})
$T_{O1} \checkmark$	$T_{A1} \times$	$T_V \checkmark$	$T_{A2} \times$	$T_{O2} \checkmark$	<i>O</i>	–Fee(T_{A1}) – Fee(T_{A2})	Revenue – Fee(T_{O1}) – Fee(T_{O2})
$T_{O1} \checkmark$	$T_{A1} \times$	$T_V \checkmark$	$T_{O2} \checkmark$	$T_{A2} \times$	<i>O</i>	–Fee(T_{A1}) – Fee(T_{A2})	Revenue – Fee(T_{O1}) – Fee(T_{O2})

TABLE VI: Adversarial payoff for a two player game. Under the assumption that both players *A* and *O* are rational, *A* “wins” the game if the front-running transaction T_{A1} is placed in front of T_{O1} , regardless of the position of the back-running transaction. A transaction that succeeds is denoted by \checkmark , while a transaction that fails, is denoted by \times .

Pct %	Latency		Provisioned	Bandwidth
	[37]	[28]	Model	Model
10	99	92	95.5	3.4
20	116	-	116	6.8
33	151	125	138	11.2
50	208	152	180	29.4
67	231	200	216	68.3
80	247	-	247	111.3
90	285	276	281	144.4
mean	209	171	181	55.0
std.	157	76	62	58.8
				52.8
				50.4

TABLE VII: Latency and bandwidth statistics from our model based on previous studies [37], [28].

b) Transaction Fees: The transaction gas price, together with the degree of blockchain transaction congestion (i.e. competing transactions that seek to be mined), influences the pace at which a transaction is mined. In our simulations, we sample the gas price of the victim transaction from a normal distribution with a mean of $(8.76 \pm 61.18 \text{ GWei})$, measured at the Uniswap DAI market from block 9M to 9.1M. We assume that the victim pays a sufficient transaction fee for its transaction to be mined in the next block. Empirical data suggests that the Ethereum average block interval time is 13.5 ± 0.12 seconds [13]. Therefore, we sample the duration of the victim’s transaction in the mempool from a uniform distribution between 0 to 30 seconds. When the network is congested, transactions on Ethereum may stay in the mempool for longer than 30 seconds, sometimes even tens of minutes [13]. However, we avoid presenting our analysis on longer pending duration, as our simulation results (cf. Figure 11 and Figure 14) show that in the case of multiple players, the adversarial transaction fee at 30 seconds is likely to render the attack unprofitable.

c) Miner: We assume the miner order transactions with descending gas prices to maximize their revenue (cf. Section VI). Besides, the miners configure a price bump percentage of 10% to replace an existing transaction from the mempool. At the time of writing, Geth (used by 78.3% of the clients) configures price bump percentage to 10%, while Parity sets 12.5%.

C. Simulation Results

Figure 11 shows the expected profit of an adversarial liquidity taker (cf. Section IV) given 2, 5, and 10 adversaries,

on the Uniswap DAI market at block 9M. The slippage of the victim transaction is fixed at 0.5%. The minimum profitable victim input is 14.75 ETH (2,197.30 USD).

We visualize the line where the expected revenue breaks even with simulated transaction costs. The transaction cost is calculated as the simulated gas price (cf. Figure 12) times the total gas consumed by the adversarial transaction. The gas consumption is randomly sampled from a normal distribution with mean at $85,488 \pm 34,782$ (taken from the Uniswap DAI market average gas consumption from block 9M to 9.1M). We observe that the break-even line grows exponentially until the victim transaction is mined (which is in line with the assumption of a 10% increase for each transaction price increase). We observe that the more adversaries, the more competitive the attack appears. For instance, our simulation suggests that the sandwich attack is not profitable after the victim transaction remained pending on the P2P network for 27.7, 20.3, 16.3 seconds, given 2, 5 and 10 adversaries respectively, when the victim *V* transacts 20 ETH for DAI. We refer the interested reader to Figure 14 for a visualization of our simulation when multiple providers attack a taker.

Our results suggest that having multiple attackers does, in expectation, divide the total revenue among the adversaries, minus the transaction fee overhead. Specifically, we find that the presence of 2, 5 and 10 attackers respectively reduce the expected profitability of the attack by 51.0%, 81.4% and 91.5% (given the victim transacts 20 ETH to DAI on Uniswap with a transaction pending on the P2P layer for 10 seconds before being mined). Note that if the blockchain is congested (i.e. T_V remains pending for more than 15 seconds), we observe that the break-even of the attacker becomes harder to attain.

VIII. RELATED WORK

Besides AMM DEX, other types of decentralised exchanges exist: limit order book based [5], [43], [39], auctions [23], trusted hardware [12], payment channel [42]. Front-running, and high frequency trading is related to the thoroughly studied problem of rushing adversaries to double-spend not yet mined blockchain transactions [35]. Strategically placed and malicious blockchain network nodes may control when and if miners receive transactions, which can affect the time at which a transaction is executed within the blockchain [44], [32], [30], [31].

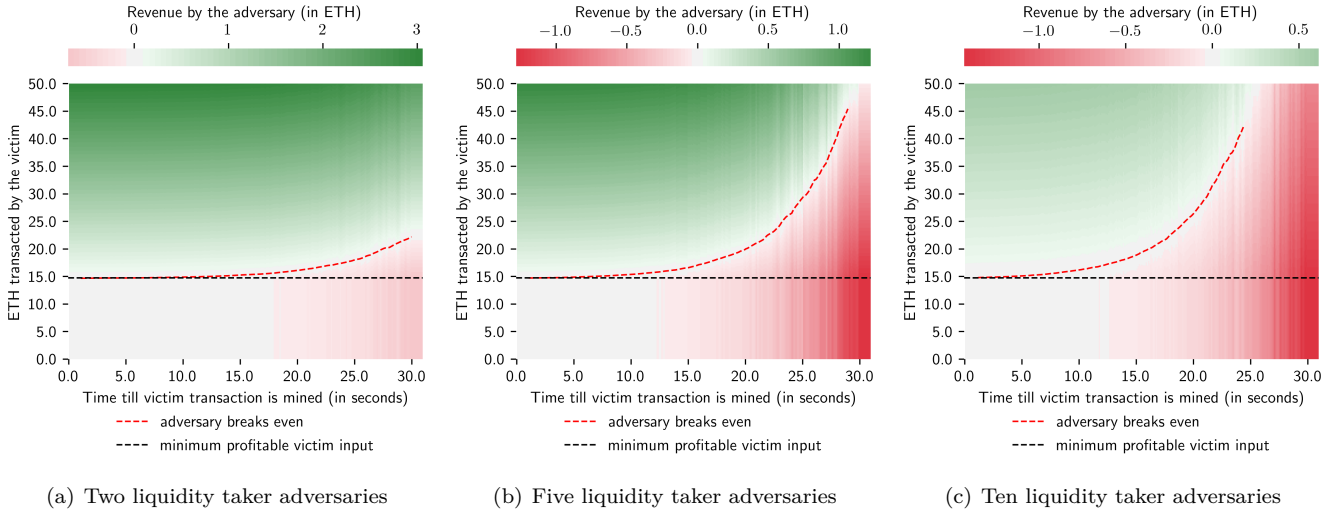


Fig. 11: Simulated sandwich attack by 2, 5 and 10 competing adversarial liquidity taker on a taker (Uniswap, block 9M, 0.3% fees, 0.5% unexpected slippage).

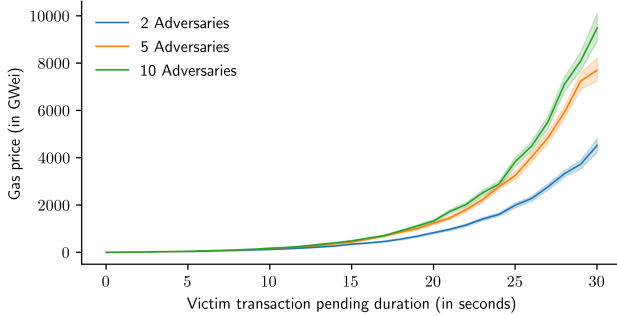


Fig. 12: The simulated gas price of the “winning” transaction when 2, 5 or 10 adversaries are performing a reactive counter-bidding attack. Each experiment is run 100,000 times. We visualize the 95% confidence interval.

The cryptographic literature captures front-running by allowing a “rushing adversary” to interact with a protocol [11]. The (financial) high-frequency trading (HFT) literature [7], [47] has also explored many trading strategies and their economic impact, such as arbitrage, news reaction strategies etc in traditional markets. Most of the traditional market strategies are also applicable to AMM and other decentralized exchanges [21], [8]. Daian *et al.* [21] in particular, introduced the concept of gas price auctions (PGA) among trading bots as well as the concept of miner extractable value (MEV). Previous studies [10] also suggest that HFT performance is strongly associated with latency and execution speed. Multiple forms of malpractice have been discovered on financial exchanges. Besides the traditional market manipulation techniques [34] (such as cornering, front-running, and pump-and-dump schemes), previous works [41] have also studied new techniques such as spoofing, pinging and mass misinformation, which

leverage modern technologies such as social media and artificial intelligence. Such techniques may even be used to trick HFT algorithms [9]. To counterbalance this inherent trust, regulators conduct periodic and costly manual audits of banks, brokers, and exchanges to unveil potential misbehavior. This is a challenging task on DEX, given weak identities, and missing regulations.

IX. CONCLUSION

In this paper, we have presented two versions of a sandwich attack, made possible by the deterministic nature of an AMM DEX in combination with the time delay inherent on on-chain exchanges. While the transparency of DEXs is desirable, it can, however, put users assets at a security risk and allow both liquidity providers and liquidity takers to exploit unknowing traders through a combination of front and back-running. Fixing such front-running is not trivial because the smaller the allowed slippage set by a trader, the more likely the trade fails. Cryptography-based defenses moreover affect the usability of the AMM DEXes due to multiple rounds of interactions or trusted off-chain components (cf. Appendix C).

We show how under multiple competing adversaries, sandwich attacks may still remain profitable. Our work, sheds light on a dilemma facing DEXs: if the default slippage is set too low, the DEX is not scalable (i.e. only supports few trades per block), if the default slippage is too high, adversaries can profit. We hope that this work draws attention to this unsolved issue and engenders future work on open, secure and decentralized finance.

ACKNOWLEDGMENTS

We very much thank the anonymous reviewers and Nicolas Christin for the thorough reviews and helpful suggestions that significantly strengthened the paper.

REFERENCES

- [1] Balancer Exchange. <https://balancer.finance/whitepaper/>.
- [2] Etherum improvement proposal 1014: Skinny create2, 2018. accessed 26 May, 2020, <https://eips.ethereum.org/EIPS/eip-1014>.
- [3] Blockchain Transparency Report, 2019.
- [4] Implementing Ethereum trading front-runs on the Bancor exchange in Python, 2019.
- [5] Kyber: An on-chain liquidity protocol. Technical report, Kyber Network, April 2019.
- [6] NASDAQ Glossary, 2019.
- [7] James J Angel and Douglas McCabe. Fairness in financial markets: The case of high frequency trading. *Journal of Business Ethics*, 112(4):585–595, 2013.
- [8] Guillermo Angeris, Hsien-Tang Kao, Rei Chiang, Charlie Noyes, and Tarun Chitra. An analysis of uniswap markets. *arXiv preprint arXiv:1911.03380*, 2019.
- [9] Jakob Arnoldi. Computer algorithms, market manipulation and the institutionalization of high frequency trading. *Theory, Culture & Society*, 33(1):29–52, 2016.
- [10] Matthew Baron, Jonathan Brogaard, Björn Hagströmer, and Andrei Kirilenko. Risk and return in high-frequency trading. *Journal of Financial and Quantitative Analysis*, 54(3):993–1024, 2019.
- [11] Donald Beaver and Stuart Haber. Cryptographic protocols provably secure against dynamic adversaries. In *Workshop on the Theory and Application of Cryptographic Techniques*, pages 307–323. Springer, 1992.
- [12] Iddo Bentov, Yan Ji, Fan Zhang, Lorenz Breidenbach, Philip Daian, and Ari Juels. Tesseract: Real-time cryptocurrency exchange using trusted hardware. In *Proceedings of the 2019 ACM SIGSAC Conference on Computer and Communications Security*, pages 1521–1538, 2019.
- [13] Bitinfocharts. Ethereum block time.
- [14] Joseph Bonneau, Edward W Felten, Steven Goldfeder, Joshua A Kroll, and Arvind Narayanan. Why buy when you can rent? bribery attacks on bitcoin consensus. 2016.
- [15] Joseph Bonneau, Andrew Miller, Jeremy Clark, Arvind Narayanan, Joshua A Kroll, and Edward W Felten. Sok: Research perspectives and challenges for bitcoin and cryptocurrencies. In *Security and Privacy (SP), 2015 IEEE Symposium on*, pages 104–121. IEEE, 2015.
- [16] Sean Bowe, Alessandro Chiesa, Matthew Green, Ian Miers, Pratyush Mishra, and Howard Wu. Zexe: Enabling decentralized private computation. *Cryptology ePrint Archive*, Report 2018/962, 2018. <https://eprint.iacr.org/2018/962>.
- [17] Lorenz Breidenbach, Phil Daian, Florian Tramèr, and Ari Juels. Enter the hydra: Towards principled bug bounties and exploit-resistant smart contracts. In *27th USENIX Security Symposium (USENIX Security 18)*, pages 1335–1352, 2018.
- [18] Benedikt Bünz, Shashank Agrawal, Mahdi Zamani, and Dan Boneh. Zether: Towards privacy in a smart contract world. *IACR Cryptol. ePrint Arch.*, 2019:191, 2019.
- [19] Raymond Cheng, Fan Zhang, Jernej Kos, Warren He, Nicholas Hynes, Noah Johnson, Ari Juels, Andrew Miller, and Dawn Song. Ekiden: A platform for confidentiality-preserving, trustworthy, and performant smart contracts. In *2019 IEEE European Symposium on Security and Privacy (EuroS&P)*, pages 185–200. IEEE, 2019.
- [20] Securities Commission and Exchange. SEC Enforcement Action Against EtherDelta. Technical report.
- [21] Philip Daian, Steven Goldfeder, Tyler Kell, Yunqi Li, Xueyuan Zhao, Iddo Bentov, Lorenz Breidenbach, and Ari Juels. Flash Boys 2.0: Frontrunning, Transaction Reordering, and Consensus Instability in Decentralized Exchanges. *arXiv preprint arXiv:1904.05234*, 2019.
- [22] Christian Decker and Roger Wattenhofer. Information propagation in the bitcoin network. In *Conference on Peer-to-Peer Computing*, pages 1–10, 2013.
- [23] DutchX, July 2019. accessed 12 November, 2019, <https://github.com/gnosis/dx-docs>.
- [24] Oğuzhan Ersoy, Zhijie Ren, Zekeriya Erkin, and Reginald L La-gendijk. Transaction propagation on permissionless blockchains: incentive and routing mechanisms. In *2018 Crypto Valley Conference on Blockchain Technology (CVCBT)*, pages 20–30. IEEE, 2018.
- [25] Shayan Eskandari, Seyedehmahsa Moosavi, and Jeremy Clark. Sok: Transparent dishonesty: Front-running attacks on blockchain. In Andrea Bracciali, Jeremy Clark, Federico Pintore, Peter B. Rønne, and Massimiliano Sala, editors, *Financial Cryptography and Data Security*, pages 170–189, Cham, 2020. Springer International Publishing.
- [26] Prastudy Fauzi, Sarah Meiklejohn, Rebekah Mercer, and Claudio Orlandi. Quisquis: A new design for anonymous cryptocurrencies. 11921:649–678, 2019.
- [27] Juan Garay, Aggelos Kiayias, and Nikos Leonardos. The bitcoin backbone protocol: Analysis and applications. In *Annual International Conference on the Theory and Applications of Cryptographic Techniques*, pages 281–310. Springer, 2015.
- [28] Adem Efe Gencer, Soumya Basu, Ittay Eyal, Robbert Van Renesse, and Emin Gün Sirer. Decentralization in bitcoin and ethereum networks. *arXiv preprint arXiv:1801.03998*, 2018.
- [29] Arthur Gervais, Ghassan O Karame, Karl Wüst, Vasileios Glykantzis, Hubert Ritzdorf, and Srdjan Capkun. On the security and performance of proof of work blockchains. In *Proceedings of the 2016 ACM SIGSAC Conference on Computer and Communications Security*, pages 3–16. ACM, 2016.
- [30] Arthur Gervais, Hubert Ritzdorf, Ghassan O Karame, and Srdjan Capkun. Tampering with the delivery of blocks and transactions in bitcoin. In *Conference on Computer and Communications Security*, pages 692–705. ACM, 2015.
- [31] Ethan Heilman, Alison Kendler, Aviv Zohar, and Sharon Goldberg. Eclipse attacks on bitcoin’s peer-to-peer network. In *24th {USENIX} Security Symposium ({USENIX} Security 15)*, pages 129–144, 2015.
- [32] Sebastian Henningsen, Daniel Teunis, Martin Florian, and Björn Scheuermann. Eclipsing ethereum peers with false friends. In *2019 IEEE European Symposium on Security and Privacy Workshops (EuroS&PW)*, pages 300–309. IEEE, 2019.
- [33] Eyal Hertzog, Guy Benartzi, and Galia Benartzi. Bancor protocol. 2017.
- [34] Robert A Jarrow. Market manipulation, bubbles, corners, and short squeezes. *Journal of financial and Quantitative Analysis*, 27(3):311–336, 1992.
- [35] Ghassan O Karame, Elli Androulaki, and Srdjan Capkun. Double-spending fast payments in bitcoin. In *Proceedings of the 2012 ACM conference on Computer and communications security*, pages 906–917. ACM, 2012.
- [36] Mahimma Kelkar, Fan Zhang, Steven Goldfeder, and Ari Juels. Order-fairness for byzantine consensus. *Cryptology ePrint Archive*, Report 2020/269, 2020. <https://eprint.iacr.org/2020/269>.
- [37] Seong Kyun Kim, Zane Ma, Siddharth Murali, Joshua Mason, Andrew Miller, and Michael Bailey. Measuring Ethereum network peers. In *Proceedings of the Internet Measurement Conference 2018*, pages 91–104. ACM, 2018.
- [38] A Kosba, A Miller, E Shi, Z Wen, and C Papamanthou. Hawk: The Blockchain Model of Cryptography and Privacy-Preserving Smart Contracts. In *IEEE Symposium on Security and Privacy*, pages 839–858, 2016.
- [39] Aurora Labs. Idex: A real-time and high-throughput ethereum smart contract exchange. Technical report, January 2019.
- [40] Kevin Liao and Jonathan Katz. Incentivizing blockchain forks via whale transactions. In *International Conference on Financial Cryptography and Data Security*, pages 264–279. Springer, 2017.
- [41] Tom CW Lin. The new market manipulation. *Emory LJ*, 66:1253, 2016.
- [42] Xuan Luo, Wei Cai, Zehua Wang, Xiuhua Li, and CM Victor Leung. A payment channel based hybrid decentralized ethereum token exchange. In *2019 IEEE International Conference on Blockchain and Cryptocurrency (ICBC)*, pages 48–49. IEEE, 2019.
- [43] MakerDAO. Intro to the oasisdex protocol, September 2019. accessed 12 November, 2019, <https://github.com/makerdao/developerguides/blob/master/Oasis/intro-to-oasis/intro-to-oasis-maker-otc.md>.

- [44] Yuval Marcus, Ethan Heilman, and Sharon Goldberg. Low-resource eclipse attacks on ethereum’s peer-to-peer network. *IACR Cryptology ePrint Archive*, 2018(236), 2018.
- [45] Vasilios Mavroudis and Hayden Melton. Libra: Fair Order Matching for Electronic Financial Exchanges. *arXiv preprint arXiv:1910.00321*, 2019.
- [46] Patrick McCorry, Alexander Hicks, and Sarah Meiklejohn. Smart contracts for bribing miners. In *International Conference on Financial Cryptography and Data Security*, pages 3–18. Springer, 2018.
- [47] Albert J Menkveld. The economics of high-frequency trading: Taking stock. *Annual Review of Financial Economics*, 8:1–24, 2016.
- [48] Satoshi Nakamoto. Bitcoin: A peer-to-peer electronic cash system. 2008.
- [49] Kaihua Qin, Liyi Zhou, Benjamin Livshits, and Arthur Gervais. Attacking the defi ecosystem with flash loans for fun and profit. *arXiv preprint arXiv:2003.03810*, 2020.
- [50] Eli Ben Sasson, Alessandro Chiesa, Christina Garman, Matthew Green, Ian Miers, Eran Tromer, and Madars Virza. Zerocash: Decentralized anonymous payments from bitcoin. In *Security and Privacy (SP), 2014 IEEE Symposium on*, pages 459–474. IEEE, 2014.
- [51] Slippage. Slippage - Investopedia, 2019.
- [52] Uniswap.io, 2018. accessed 12 November, 2019, <https://docs.uniswap.io/>.
- [53] Gavin Wood. Ethereum: A secure decentralised generalised transaction ledger. *Ethereum Project Yellow Paper*, 2014.
- [54] Jiahua Xu and Benjamin Livshits. The anatomy of a cryptocurrency pump-and-dump scheme. In *28th USENIX Security Symposium (USENIX Security 19)*, pages 1609–1625, 2019.

APPENDIX A SANDWICH ATTACK DETAILS

In what follows, we assume that a victim V sends a transaction T_V to trade δ_x^V of X for δ_y^V of Y . The underlying AMM market starts with the initial state $s_0 = (x_0, y_0)$. Eq. 6 shows the transition in AMM state after applying T_V without unexpected slippage.

$$s_0 \xrightarrow{\text{TransactXForY}(\delta_x^V)} (x^*, y^*), \quad \delta_y^V = y_0 - y^* \quad (6)$$

$$x^* = x_0 + \delta_x^V, \quad y^* = \frac{x_0 y_0}{x_0 + \delta_x^V - c_x(s_0, \delta_x^V)} + c_y(s_0, \delta_y^V) \quad (7)$$

A. Liquidity Taker Attacks Taker

We assume that the adversary A has an initial state $(\delta_x^{A1}, 0)$, and attacks by emitting T_{A1} and T_{A2} .

T_{A1} : a front-running transaction, exchanges δ_x^{A1} for δ_y^{A1} of Y and is planned to execute before T_V (e.g. by paying a higher transaction fee than T_V). This results in the state changes of Equation 8 and 9.

$$s_0 \xrightarrow{\text{TransactXForY}(\delta_x^{A1})} s_1 = (x_1, y_1), \quad \delta_y^{A1} = y_0 - y_1 \quad (8)$$

$$x_1 = x_0 + \delta_x^{A1}, \quad y_1 = \frac{x_0 y_0}{x_1 - c_x(s_0, \delta_x^{A1})} + c_y(s_0, \delta_y^{A1}) \quad (9)$$

T_V : a victim transaction modifies the state as per Equation 10 and 11.

$$s_1 \xrightarrow{\text{TransactXForY}(\delta_x^V)} s_2 = (x_2, y_2), \quad \delta_y^V = y_1 - y_2 \quad (10)$$

$$x_2 = x_1 + \delta_x^V, \quad y_2 = \frac{x_1 y_1}{x_2 - c_x(s_1, \delta_x^V)} + c_y(s_1, \delta_y^V) \quad (11)$$

T_{A2} : a back-running transaction exchanges $\delta_y^{A2} = \delta_y^{A1} - c_y(s_2, \delta_y^{A2})$ for δ_x^{A2} of X and is planned to execute after T_V (e.g. by paying a lower transaction fee than T_V). T_{A2} effectively closes the adversary’s position that was opened by T_{A1} (cf. Equation 12 and 13).

$$s_2 \xrightarrow{\text{TransactXForY}(\delta_y^{A2})} s_3 = (x_3, y_3), \quad \delta_x^{A2} = x_2 - x_3 \quad (12)$$

$$x_3 = \frac{x_2 y_2}{y_3 - c_y(s_2, \delta_y^{A2})} + c_x(s_0, \delta_y^{A2}), \quad y_3 = y_2 + \delta_y^{A2} \quad (13)$$

Transaction T_{A2} swaps the asset Y from transaction T_{A1} in exchange for asset X . The corresponding profit is determined by comparing the input from T_{A1} and the output T_{A2} of asset X (cf. Equation 14).

$$\text{profit} = \delta_x^{A2} - \delta_x^{A1} \quad (14)$$

After the attack, the state of adversary becomes $(\delta_x^{A2}, 0)$. Thus, provided the profit exceeds the costs (e.g. transaction fees and equipment costs), a rational adversary would undertake the attack.

B. Liquidity Provider Attacks Taker

We use (x_N, y_N) to denote the state of an AMM exchange at block $N \in \mathbb{Z}$, where x_N, y_N are the amounts of asset X and Y in the liquidity pool (cf. Definition 1). The liquidity provider owns a share of $L \in [0, 1]$ liquidity if it deposits $\delta_{x,N} = x_N \frac{L}{1-L}$ of asset X and $\delta_{y,N} = y_N \frac{L}{1-L}$ of asset Y into the liquidity pool. We use $Z_N(x, y)$ to denote the USD value of assets at block N , where x is the amount of asset X and y is the amount of asset Y . Given two blockchain blocks m, n , where the respective AMM states differ, the deposit of $z_m = Z_m(x_m \frac{L}{1-L}, y_m \frac{L}{1-L})$ at block m , or $z_n = Z_n(x_n \frac{L}{1-L}, y_n \frac{L}{1-L})$ at block n both results in a share of L liquidity in the respective market X/Y . For the following section, we set $z_m > z_n$.

1) Attack Profitability: We proceed by defining profitability for an adversary. $L_x, L_x^*, L_y, L_y^* \in [0, 1]$ denote the proportion of assets X and Y held by the adversary in the liquidity pools before and after the attack. Analogously, $x^A, x^{A*}, y^A, y^{A*} \in \mathbb{Z}^+$ denote the amounts of asset X and Y held by the adversary before and after the attack.

$$(L_x, L_y, x^A, y^A) \xrightarrow{\text{attack}} (L_x^*, L_y^*, x^{A*}, y^{A*}) \quad (15)$$

The state transition (cf. Equation 15) is profitable to the adversary, if the following conditions hold:

- $L_x^* \not\propto L_x, \quad L_y^* \not\propto L_y, \quad x^{A*} \not\propto x^A, \quad y^{A*} \not\propto y^A, \quad$ and
- At least one of the following holds:
 $L_x^* > L_x, \quad \text{or} \quad L_y^* > L_y, \quad \text{or} \quad x^{A*} > x^A, \quad \text{or} \quad y^{A*} > y^A$

Let x^* and y^* denote the amounts of asset X and Y in liquidity pools after the attack. The corresponding profit

is determined by comparing adversary's states before and after the attack (cf. Equation 16, 17, 18).

$$\Delta_x^A = x^{A*} - x^A + (L_x^* - L_x)x^* \quad (16)$$

$$\Delta_y^A = y^{A*} - y^A + (L_y^* - L_y)y^* \quad (17)$$

$$\text{profit} = Z(\Delta_x^A, \Delta_y^A) \quad (18)$$

2) *Attack Execution:* We now consider an adversarial liquidity provider that owns a share $L_x x_0, L_y y_0$ of the total liquidity pool of a AMM X/Y market. The victim's transaction T_V transacts asset X for Y . If the adversary does not front-run T_V , the AMM state changes according to Equation 19, 20. In that case, the adversary A receives a commission fee c , as stated in Equation 21, 22.

$$s_0 \xrightarrow{\text{TransactXForY}(\delta_x^V)} s_1 = (x_1, y_1), \quad \delta_y^V = y_0 - y_1 \quad (19)$$

$$x_1 = x_0 + \delta_x^V, \quad y_1 = \frac{x_0 y_0}{x_1 - c_x(s_0, \delta_x^V)} + c_y(s_0, \delta_x^V) \quad (20)$$

$$c_x^{A,T_V} = L \times c_x(s_0, \delta_x^V), \quad c_y^{A,T_V} = L \times c_y(s_0, \delta_x^V) \quad (21)$$

$$(L_x, L_y, x^A, y^A) \rightarrow (L_x, L_y, x^A + c_x^{A,T_V}, y^A + c_y^{A,T_V}) \quad (22)$$

This liquidity provider attempts to gain a profit through the following order of transactions.

T_{A1} : a front-running transaction executed before T_V (e.g. by paying a higher transaction fee than T_V). T_{A1} withdraws $(L_x x_0, L_y y_0)$ from the liquidity pool (x_0, y_0) and results in the state changes of Equation 23 and 24.

$$s_0 \xrightarrow{\text{RemoveLiquidity}(L_x x_0, L_y y_0)} s_1 = (x_1, y_1) \quad (23)$$

$$x_1 = x_0 - L_x x_0, \quad y_1 = y_0 - L_y y_0 \quad (24)$$

T_V : a victim's transaction modifies the state according to Equation 25 and 26.

$$s_1 \xrightarrow{\text{TransactXForY}(\delta_x^V)} s_2 = (x_2, y_2), \quad \delta_y^V = y_1 - y_2 \quad (25)$$

$$x_2 = x_1 + \delta_x^V, \quad y_2 = \frac{x_1 y_1}{x_2 - c_x(s_1, \delta_x^V)} + c_y(s_1, \delta_x^V) \quad (26)$$

T_{A2} : a back-running transaction executes after T_V (e.g. by paying a lower transaction fee than T_V). T_{A2} adds back liquidity for the adversary to maintain the same proportion of overall liquidity (L_x, L_y) , modifying the state according to Equation 27 and 28.

$$s_2 \xrightarrow{\text{AddLiquidity}(\frac{L_x x_2}{1-L_x}, \frac{L_y y_2}{1-L_y})} s_3 = (x_3, y_3) \quad (27)$$

$$x_3 = \frac{x_2}{1-L_x}, \quad y_3 = \frac{y_2}{1-L_y} \quad (28)$$

T_{A3} : executed after T_{A2} , T_{A3} rebalances the AMM assets by converting Y to X , such that the adversary retains the same amount of asset X as before the attack (i.e. the adversary holds $x^A + c_x^{A,T_V}$ after the attack). This

rebalancing process is necessary because the amount of asset X added to liquidity pool in T_{A2} exceeds the amount withdrawn from T_{A1} . T_{A3} modifies the state according to the Equations 29, 30 and 31.

$$s_3 \xrightarrow{\text{TransactXForY}(\delta_y^{A3})} s_4 = (x_4, y_4), \quad \delta_x^{A3} = x_3 - x_4 \quad (29)$$

$$x_4 = \frac{x_3 y_3}{y_4 - c_y(s_3, \delta_y^{A3})} + c_x(s_3, \delta_y^{A3}), \quad y_4 = y_3 + \delta_y^{A3} \quad (30)$$

$$\delta_x^{A3} = \frac{L_x x_2}{1-L_x} + c_x^{A,T_V} - L_x x_0 \quad (31)$$

The overall state change of this attack is described in Equation 32. At the end of this attack, the adversary A has managed to retain L proportion of the total liquidity as a result of T_{A2} , retains the same total amount of asset X (as a result of T_{A3}) but increases their holding of asset Y , generating a profit. Equation 33 yields the profit.

$$(L_x, L_y, x^A, y^A) \xrightarrow{\text{attack}} (L_x, L_y, x^A + c_x^{A,T_V}, y^{A*}) \quad (32)$$

$$\text{profit} = y^{A*} - (y^A + c_y^{A,T_V}) \quad (33)$$

APPENDIX B ADDITIONAL DETAILS FOR LIQUIDITY PROVIDER

Figure 13 quantifies the optimal adversarial revenue by a liquidity provider, given no other attacks are running.

Figure 14 shows the expected profit of an adversarial liquidity provider (cf. Section IV) given 2, 5, and 10 adversaries, on the Uniswap DAI market at block 9M. The victim transaction is fixed with a 0.5% slippage protection. The minimum profitable victim input with a single adversary is 27.8 ETH (4,141.37 USD).

APPENDIX C POSSIBLE MITIGATIONS

In this section we elaborate on how users could protect their trades from sandwich attacks, and we discuss possible AMM design changes to strengthen their resilience.

A. AMM Specific Settings

We identify two primary protection possibilities that could be adopted given the existing AMM DEX designs (such as Uniswap).

1) *Allow for Zero Slippage:* The simplest protection for a user, is to not allow its trades to pay any slippage. If an adversary were to front-run, the user's trade execution will fail. The user would not overpay the trade due to its slippage protection, but the user still is liable to pay blockchain transaction fees. This protection solution moreover is not scalable in terms of trades per second, as it would limit the number of trades an AMM DEX can execute to 1 transaction per blockchain block.

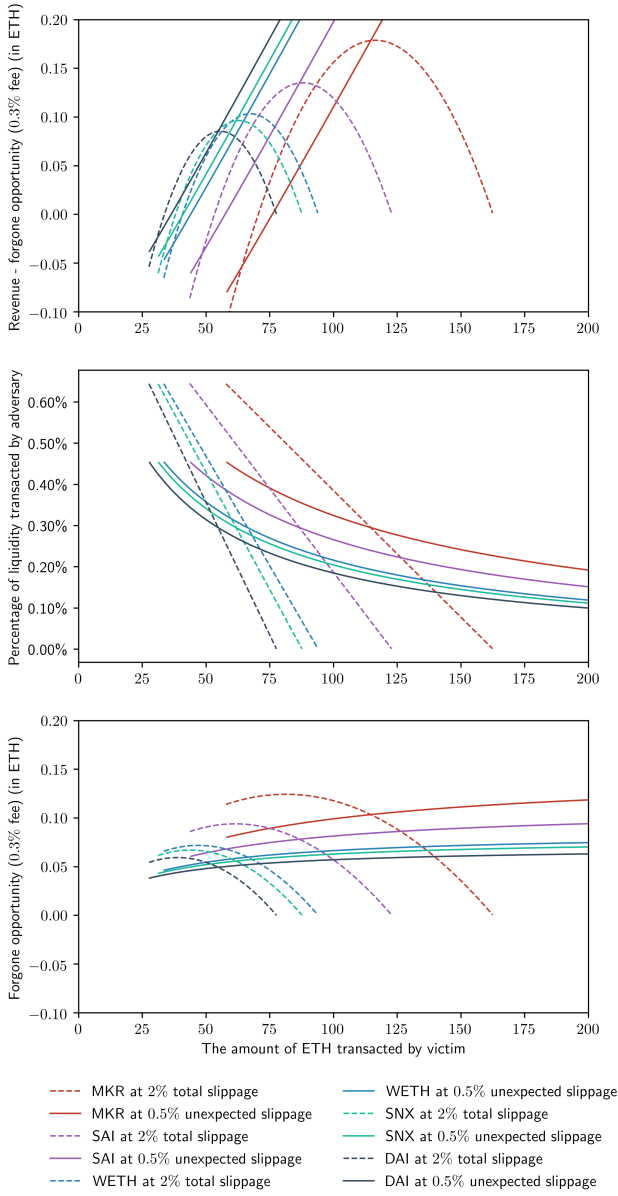


Fig. 13: Optimal adversarial revenue under a sandwich attack by a liquidity provider, when V sells assets for ETH on five Uniswap exchanges (0.3% fee, adversarial break-even at 0.01 ETH).

2) *Limit Liquidity Taker's Input:* Recall that sandwich attacks are only profitable if the victim's input amount is above a threshold, which we named it as the minimum profitable victim input (cf. Section IV). This threshold depends on both the total liquidity of the market and the AMM DEX's design and configuration (pricing formula, fees and etc.). One possible protection is to disable transactions above the minimum profitable victim input in the smart contracts.

B. Cryptography-based Defences

In the following we discuss possible cryptography based defence techniques against sandwich attacks.

1) *Multi-Party Computation (MPC):* The sandwich attack is possible because the current consensus protocol used in Ethereum fails to protect the actual ordering of the transactions from adversarial manipulations (i.e. fee manipulations). Thus, it is tempting for one to design an AMM DEX that has a authorized set of “trusted” nodes to faithfully sequence actions from liquidity takers before getting the actions executed by the smart contract. This proposal, however, makes AMM DEX like Uniswap no longer permissionless, and the authorized set can again manipulate the order of the transactions. To address the later, Kelkar *et al.* [36] propose a new set of Byzantine Consensus protocols, that achieve a fair ordering of received transactions. Thus, one can require the authorized set of nodes to run such protocol to achieve order fairness among transactions.

2) *Commit-and-Reveal Protocols:* A commitment scheme is a two-round protocol that allows one to commit to chosen values (i.e. function, input) while keeping those values hidden from others (*hiding*) during the committing round, and later during the revealing round, s/he can decide to reveal the committed value. The commitment schemes are *binding* if and only if the party cannot change the value after committing to it. We briefly discuss the use of commitment scheme to prevent front-running in the following.

a) *Standard Commit-and-Reveal Protocol:* To prevent the sandwich attack in AMM DEX, one can use commitment schemes to sequence actions of traders during committing round and execute actions during revealing round. In particular, during committing round, traders commit to function calls (i.e. `TransactXforY`, `addLiquidity`, `removeLiquidity`) via commitment transactions, and the ordering of function calls is determined based on the order of commitments while the function calls are hidden due to the *hiding* property of a commitment scheme. In the revealing round, parties can decide to reveal the function calls, and the AMM DEX will execute the transactions according to the order of the commitments appeared in the committing round.

One of the limitations of commit-and-reveal protocol is its usability, as it requires participants to be aware of both rounds of the protocol to complete their actions. Another limitation is that adversary is still able to *probabilistically* perform sandwich attack. In particular, because the committing round is transparent, the adversary can see other traders' commitments and commits several transactions before and after the commitments of honest traders. S/he can reveal only those transactions that are profitable.

b) *Commit-and-Reveal Protocol tailored for the Ethereum Blockchain:* To hide the committing phase from the adversary, Breidenbach *et al.* [17] proposed submarine commitments via contract creation in Ethereum (i.e.

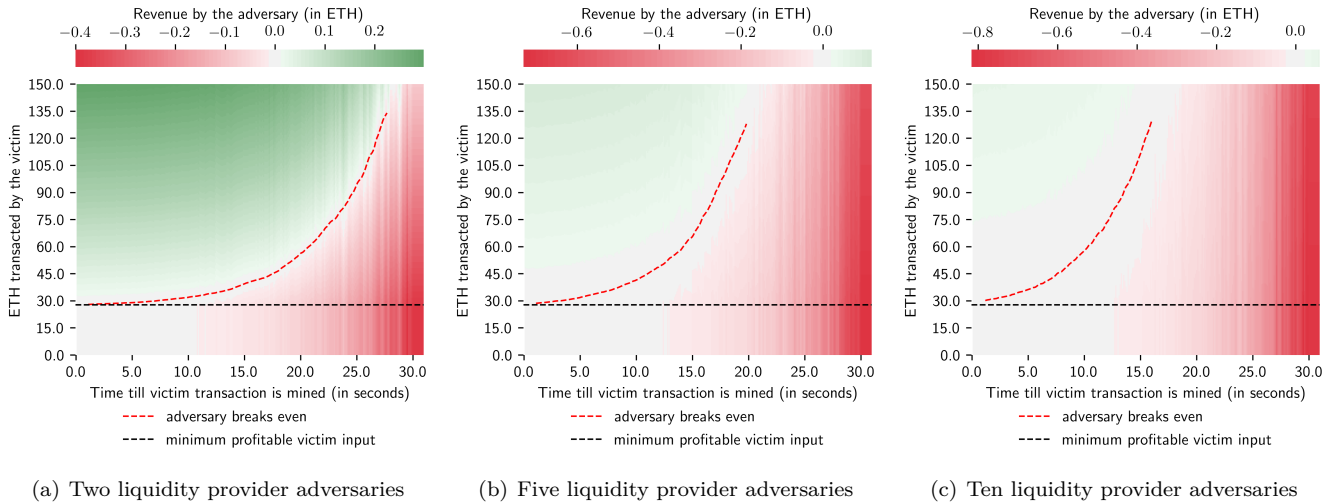


Fig. 14: Simulated sandwich attack by 2, 5 and 10 competing adversarial liquidity provider on a taker (Uniswap, block 9M, 0.3% fees, 0.5% unexpected slippage).

CREATE2 EVM opcode [2]). The essence of this approach is to hide commitment transaction among newly generated Ethereum addresses. In particular, a submarine commitment scheme contains the following phases:

Committing Phase: to *commit* in a submarine commitment scheme, the liquidity taker with address $\text{Addr}_{\text{Taker}}$ posts a transaction T_{com} that sends some fund, val , to an address Addr_{com} . Addr_{com} is a commitment of the form:

$$\text{Addr}_{\text{com}} = H(\text{Addr}_{\text{AMM-DEX}}, H(\text{Addr}_{\text{Taker}}, \text{key}), \text{code})$$

where $H(\cdot)$ is Keccak-256, key is the transaction specific key to AMM DEX (e.g. a concatenation of action transactXforY , input δ_x , and 256-bit randomness r), and code is the EVM init code of the *refund* contract that can send any money received to the $\text{Addr}_{\text{AMM-DEX}}$.

Revealing Phase: To reveal, $\text{Addr}_{\text{Taker}}$ sends to $\text{Addr}_{\text{AMM-DEX}}$, key value $\text{key} = (\text{action} || \text{input} || r)$, the transaction data T_{com} , the *commitBlock* (the block number includes T_{com}), and a Merkle-Partricia proof, $\pi_{T_{\text{com}}}$ which proves the membership of T_{com} in *commitBlock*. With *commitBlock*, $\pi_{T_{\text{com}}}$, and T_{com} , $\text{Addr}_{\text{AMM-DEX}}$ verifies that T_{com} occurred in *commitBlock*. And after learning key , $\text{Addr}_{\text{AMM-DEX}}$ can recompute Addr_{com} , verifies the deposit balance val , and proceeds with *action* and *input* (i.e. $\text{transactXforY}(\delta_x)$).

Deposit Collection Phase: from code , $\text{Addr}_{\text{AMM-DEX}}$ can use CREATE2 opcode to create an instance of the *refund* contract at Addr_{com} and collect $\$val$ from Addr_{com} .

3) *Confidential Transactions:* Another potential attempt to mitigate front-running attack is to hide the details of the transaction sent to AMM DEX by adapting several techniques [50], [18], [16], [26] for confidential transactions. However, as pointed out by Eskandari et al. [25], to prevent front-running, one needs to hide:

- (1) The name of the functions (i.e. TransactXforY ,

- addLiquidity, removeLiquidity) being invoked
- (2) The parameters supplied to the functions (i.e. δ_x, δ_y)
- (3) The current state of the DEX (i.e. (x, y)).

While systems like Hawk [38] and Ekiden [19] try to achieve all three properties for arbitrary functions, they rely on off-chain components (i.e. trusted execution environment) for maintaining encrypted states and proving the correctness of state transitions. On the other hand, a proposal for Ethereum blockchain, Zether [18], tries to achieve (2, 3) for a specific type of function (i.e. money transferring). The states in Zether are the ElGamal encryptions of account's balances. The state transitions can be made due to the correctness of the non-interactive zero-knowledge proof (NIZK) system used in their construction and the (additively) homomorphic properties of Elgamal encryption.

However, recall that in an AMM DEX, an action like $\text{TransactXforY}(\delta_x)$ requires the contract to send an δ_y of asset Y back to the liquidity taker where δ_y is computed based on the pricing function $f(\cdot)$ and the current pool's state (x, y) . Therefore, if one decides to use a system that relies on NIZK systems like Zether for AMM DEX with hidden state, the trusted off-chain components are needed to generate cryptographic proofs from the unencrypted state to trigger the transferring back function.

Moreover, regardless of the privacy techniques used for hiding transaction details and pool's states, we show that it is impossible to achieve the confidentiality for the third property for a constant product AMM. In particular, at the initial pool state $s = (x, y)$, an adversary can issue two consecutive actions, $\text{TransactXforY}(\delta_x)$, $\text{TransactXforY}(\delta'_x)$, and it obtains δ_y and δ'_y determined by the current state (x, y) . The adversary can solve the system of two equations and two unknown (x, y) to determine the current pool state.